EFFECT OF NITROGEN DOPING ON THE STRUCTURAL AND OPTICAL PROPERTIES OF Zn_2GeO_4 PHOSPHORS

N. M. C. H. P. Lan [1*], D. V. Tuan [1], T. Q. Tuan [1], N. D. T. Kien [1], C. X. Thang [1*], N. V. Tung [2], N. T. Giang [3]

[1] Advanced Institute for Science and Technology (AIST), Hanoi University of Science and Technology (HUST), Hanoi, Vietnam; e-mail: thang.caoxuan@hust.edu.vn, mc@180995@gmail.com
[2] Institute of Science and Technology, Ministry of Public Security, Hanoi, Vietnam
[3] Department of Chemistry, Faculty of Materials, Hanoi University of Civil Engineering, Hanoi, Vietnam

Nitrogen-doped Zn_2GeO_4 (ZGO:N) phosphors were synthesized using a chemical hydrothermal approach. The influence of nitrogen doping on the structural and optical properties of ZGO phosphors was investigated. Results indicated that N ions substituted for O ions successfully and N doping expanded throughout the unit cell of the crystal host lattice. We observed a slight blue-shift in bandgap energy, which signified the weak quantum confinement of the prepared ZGO nanoparticles. At a 260-nm excitation wavelength, compared with the photoluminescence (PL) spectrum of the ZGO phosphors, the peak position of emission of the N-doped ZGO phosphors blue shifted. In the vibrational modes of ZGO owing to N incorporation, H substituted at the O site, subsequently causing passivation in ZGO:N nanoparticles. The concentration of N ions in ZGO:N played important roles in the evolution of PL intensity and quality of nanocrystals. This result contributed to the optimization of nitrogen-doped phosphors with 5 mol% content. The possible luminescence mechanism of ZGO:N phosphors was also discussed.

Keywords: *Zn_2GeO_4 phosphors, nitrogen-doped, hydrothermal method.*

ВЛИЯНИЕ ЛЕГИРОВАНИЯ АЗОТОМ НА СТРУКТУРНО-ОПТИЧЕСКИЕ СВОЙСТВА ЛЮМИНОФОРОВ Zn_2GeO_4

N. M. C. H. P. Lan [1*], D. V. Tuan [1], T. Q. Tuan [1], N. D. T. Kien [1], C. X. Thang [1*], N. V. Tung [2], N. T. Giang [3]

УДК 535.37:546.17

[1] Передовой институт науки и технологий Ханойского университета науки и технологии, Ханой, Вьетнам; e-mail: thang.caoxuan@hust.edu.vn, mc@180995@gmail.com
[2] Институт науки и технологий Министерства общественной безопасности, Ханой, Вьетнам
[3] Ханойский университет гражданского строительства, Ханой, Вьетнам

(Поступила 1 апреля 2021)

Легированные азотом люминофоры Zn_2GeO_4 (ZGO:N) синтезированы с использованием химического гидротермального подхода. Исследовано влияние легирования азотом на структурные и оптические свойства люминофоров ZGO. Показано, что ионы азота успешно заменяют ионы кислорода и легирование азота распространяется по всей элементарной ячейке кристаллической решетки. Небольшое синее смещение энергии запрещенной зоны указывает на слабое квантовое удержание полученных наночастиц ZGO. При длине волны возбуждения 260 нм по сравнению со спектром фотолюминесценции люминофоров ZGO положение максимума излучения люминофоров ZGO, легированных азотом, смещается в синюю область. В колебательных режимах ZGO из-за включения азота водород замещается в О-сайте, что вызывает пассивацию в наночастицах ZGO:N. Концентрация ионов азота в ZGO:N играет важную роль в эволюции интенсивности фотолюминесценции и качества нанокристаллов. Результат способствует оптимизации легированных азотом люминофоров с содержанием 5 мол.%. Обсуждается возможный механизм люминесценции люминофоров ZGO:N.

Ключевые слова: *люминофоры Zn_2GeO_4, легирование азотом, гидротермальный метод.*

Introduction. Zinc orthogermanate (ZGO) is a phosphor with bluish-white luminescence and a wide bandgap of 4.68 eV. ZGO materials have good thermal stability, nontoxicity and high brightness, i.e., they are 40% brighter than commercial phosphors of ZnO [1, 2]. ZGO as an important p-block metal oxide with d^{10} configuration is a type of glass or ceramic with special optical properties [3]. The optical properties of ZGO are still of special interest, and the emission of ZGO changes with two main factors: the method of fabrication and the ion doping. Under excitation with ultraviolet and near-ultraviolet light, the ZGO phosphor emits a broad band from blue to red [4]. Many papers have been published on ZGO materials doped with rare-earth (RE) and transition metals and show excellent luminescent properties [5–9]. Guoping Dong and colleagues successfully synthesized ZGO:Mn^{2+} through an easy solvothermal method. These phosphors can be applied in lighting, optical displays, and optoelectronic devices [10]. PanLai Li's group researched and manufactured ZGO:Cr^{3+} materials by a solid-phase reaction and used the product to make phosphor powder [11]. Zhijun Wang and colleagues successfully researched and manufactured ZGO:RE materials (RE: Ce^{3+}, Eu^{3+}, Tb^{3+}, and Dy^{3+}) for application as phosphor powder [12]. To date, no study has focused on the optical properties, structural morphology, and effect of nitrogen anion concentration on ZGO:N phosphors synthesized using the hydrothermal method. Notably, studying the phase and morphological structures affect the optical properties of materials. Driven by the aforesaid motivations, we aimed to understand the effect of nitrogen doping on the structural and optical properties of ZGO nanoparticles. N-doped ZGO (ZGO:N) nanoparticles were prepared with various dopant concentrations using a hydrothermal method. The samples were subjected to a series of characterizations, and the results were systematically discussed.

Experimental. All samples with composition ZGO:*x* mol% N (*x* = 0–9) were synthesized using a hydrothermal method. All chemical reagents, including GeO_2 (99.99%), $Zn(CH_3COO)_2 \cdot 2H_2O$ (>98%), $CO(NH_2)_2$ (AR), and NaOH (AR) used in this experiment were purchased from Sigma-Aldrich.

The N-doped ZGO samples were synthesized using a simple hydrothermal method. In the synthesis of one of the solutions, GeO_2 (1 mmol), NaOH (2 mmol), and $CO(NH_2)_2$ (0–0.09 mmol) were added to a mixture of 10 mL of deionized water. The process of mixing ends after the GeO_2 powder is completely dissolved. The second solution synthesis contained $Zn(CH_3COO)_2 \cdot 2H_2O$ (2 mmol) and 20 mL of deionized water. After stirring the mixture to form a homogeneous solution, additional agitation was conducted for 60 min, and then the solution was transferred to an 80-mL stainless Teflon-lined autoclave, sealed, and maintained at 200°C for 24 h. After cooling to room temperature, the as-obtained precipitate (ZGO:*x* mol% N) was washed several times with deionized water and ethanol and dried in a vacuum-drying oven. The powders were dried at 80°C several times.

The crystalline structures of ZGO:N were characterized by X-ray diffraction (XRD; D8 Advance; Bruker, Germany) with CuK_α radiation (λ = 1.5418 Å and 2θ = 10–70°). The morphologies of samples were investigated by field-emission scanning electron microscopy (FESEM; JEOL, JSM-6700F, JEOL Techniques, Tokyo, Japan) accompanied by energy-dispersive spectroscopy to examine the chemical composition. Photoluminescence (PL) measurements were performed to evaluate the optical properties of nitrogen-doped ZGO. A NANO LOG spectrofluorometer (Horiba, USA) equipped with a 450-W Xe arc lamp and double-excitation monochromators were used. All samples were investigated using a PMS-80 UVVISNEAR IR spectroscopy analysis system of ZGO and ZGO:N phosphor.

Results and discussion. Figure 1a shows the XRD patterns of *x* mol.% N-doped ZGO powder samples (*x* = 0–9), recorded within the 2θ range of 10–70°. Prominent XRD lines were observed at (110), (300), (220), (113), (410), (223), (600), (520), (333), (603), (523), (710), (006), (630), (713), (550), (633), and (416). These lines were indexed accordingly, and all diffraction peaks of the samples can be assigned to a pure rhombohedral ZGO phase (JCPDS No. 11-0687) [13]. No extra peak was observed in the XRD patterns from the N-doped samples, suggesting that the N ion was completely substituted in the ZGO lattice. A close evaluation of the XRD peaks from 30° (113) to 35° (410) in Fig. 1b shows that the diffraction peaks of the N-doped sample were located at a higher angle than the ZGO host. A higher concentration of nitrogen doping corresponded with a greater increase in peak diffraction to a higher angle. This peak deviation can be explained as follows. Given that the ionic radii of N (r_N^{2+} = 1.46 Å) is greater than that of O (r_O^{2+} = 1.38 Å), the N substitution for O in the ZGO lattice may result in tensile strain with expanded crystallite size [14]. We calculated the lattice constants, cell parameters, and volume of ZGO:*x* mol.% N by using the formula [15]:

$$1/d^2 = \frac{4}{3}\left(\frac{h^2 + hk + k^2}{a^2}\right) + \frac{l^2}{c^2}, \quad (1)$$

$$V = a^2 c(\sqrt{3}/2), \quad (2)$$

where h, k, l are Miller factors, $\lambda = 1.5418$ Å is the wavelength of the X-ray, and 2θ is the diffraction angle. In the (113) and (223), the lattice parameters a, c, and V of ZGO:x mol.% N with different doping rates were calculated and presented in Table 1. Obviously, changes occurred in cell parameters a, c, and V of ZGO base materials when doped with N ion. A greater deviation led to a higher N ion-doping concentration. The C values are presented in Table 1. With increased N doping, the lattice constant C increased from 9.5105 to 9.5252 Å. The lattice parameters can be expected when N ions are replaced by O ions; thus, the substitution of N dopant resulted in the modification of the lattice constant C. The above result led to greatly increased cell parameters and volumes for ZGO:x mol.% N. Thus, N-doped ZGO phosphors were synthesized by substituting the O site.

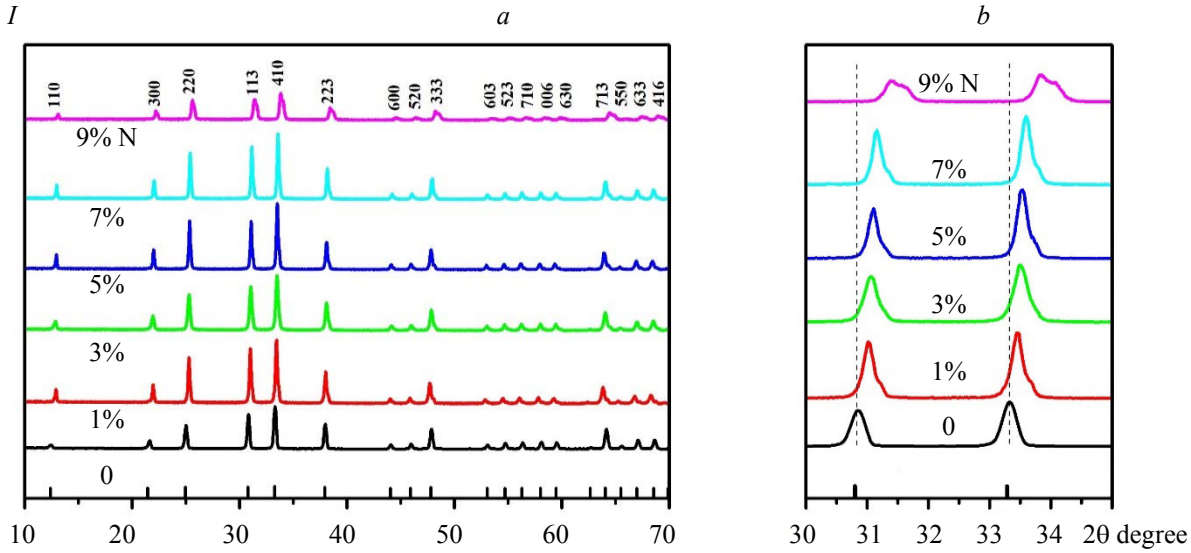

Fig. 1. (a) XRD patterns of ZGO and ZGO:x mol.% N (x = 0–9) nanophosphors, and (b) partially enlarged detail of the (113) and (410) peaks prepared using a hydrothermal method at 200°C for 2 h.

TABLE 1. Crystallographic Data of ZGO:N

Parameter	ZGO	ZGO:1%N	ZGO:3%N	ZGO:5%N	ZGO:7%N	ZGO:9%N
a, Å	14.2133	14.2115	14.2242	14.2279	14.2336	14.2346
c, Å	9.5105	9.5111	9.5114	9.5136	9.5203	9.5252
V, Å^3	1663.88	1665.91	1666.59	1667.85	1670.36	1671.45

Having determined the phase and basic crystal parameters, FESEM was used to ascertain the morphology of undoped and N-doped ZGO. The morphologies of the prepared ZGO:x mol.% N (x = 0–9) nanostructures are shown in Fig. 2. The lattice fringes of nanostructures through FESEM images are also shown in the respective inset figures. With increased doping concentration, the size of ZGO nanoparticles increased. The nanoparticle sizes estimated through FESEM analysis were also in line with the XRD analysis results. The modal nanoparticle size of doped samples was larger than that of undoped samples. In fact, the moral values of nanoparticles slightly increased with increased light intensity, confirming the incorporation of N dopants into undoped ZGO nanoparticles.

To demonstrate the ability of N ions to enter the ZGO lattice, we also investigated the phosphor properties through UV-Vis spectroscopy analysis. Figure 3a shows that the optical absorption margin of ZGO:N slightly shifted to the higher-energy region than ZGO (4.66 eV). We found that with increased doping concentration, the bandgap of ZGO phosphor increased (4.7 eV). This bandgap was due to the size-confinement effect for nanoparticles [16]. In the present case, the energy gap increased to higher valance owing to the impurity levels of N. This result further demonstrated the successful doping of nitrogen ion into the ZGO host lattice.

To determine the presence or absence of molecular species in the prepared nanoparticles and subsequently detect the influence of N doping on the vibrational modes of ZGO nanoparticles, the FTIR transmission-

mode spectra for undoped and ZGO:N nanoparticles were recorded, and the results are shown in Fig. 3b. The IR modes at 420, 520, 730, and 800 cm^{-1} were attributed to the vibration modes of ZnO_4 and GeO_4 tetrahedra in Zn_2GeO_4 [17]. An additional IR peak at 906 cm^{-1} was observed for N-doped ZGO, i.e., 1 to 9 mol.% N doping (Fig. 3b). The vibrational mode at 906 cm^{-1} was related to substitutional hydrogen to an oxygen site (H_O) bound to the lattice Zn site (i.e., Zn-H_O). This substitutional hydrogen may act as a shallow donor in ZGO. This peak evidently indicates the passivation of ZGO:N by H, as H preferred to bind with N_O at the antibonding forms N_O-H complex. This finding further confirmed the substitution of O by N in the ZGO host lattice [18].

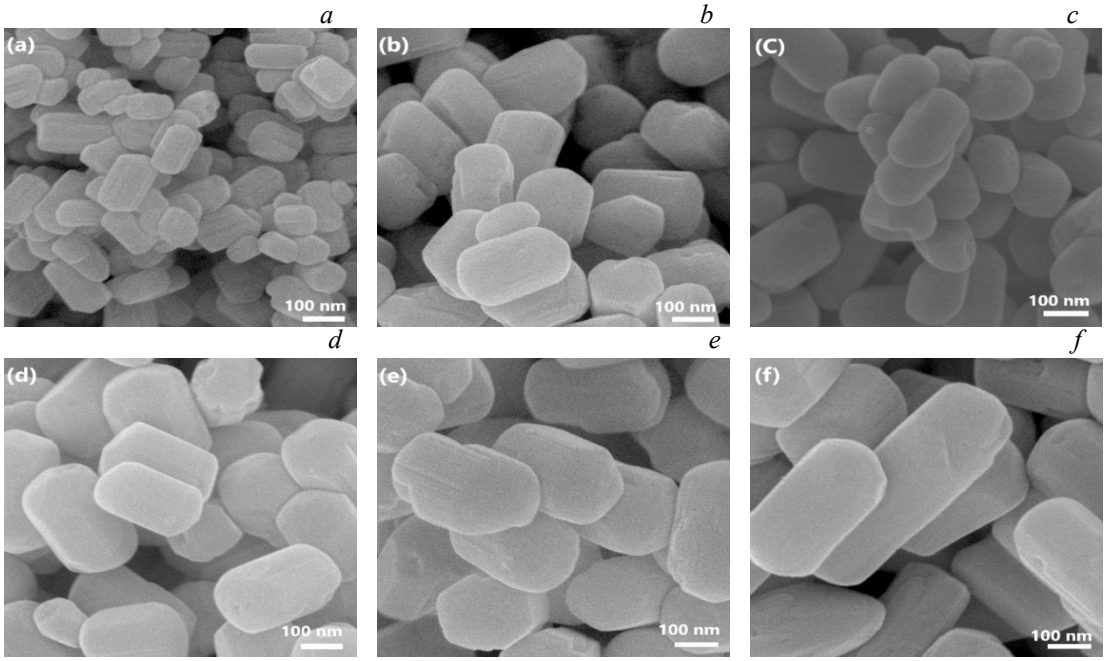

Fig. 2. FESEM of ZGO:*x* mol.% N (*x* = 0–9) nanophosphors prepared using a hydrothermal method at 200°C for 2 h.

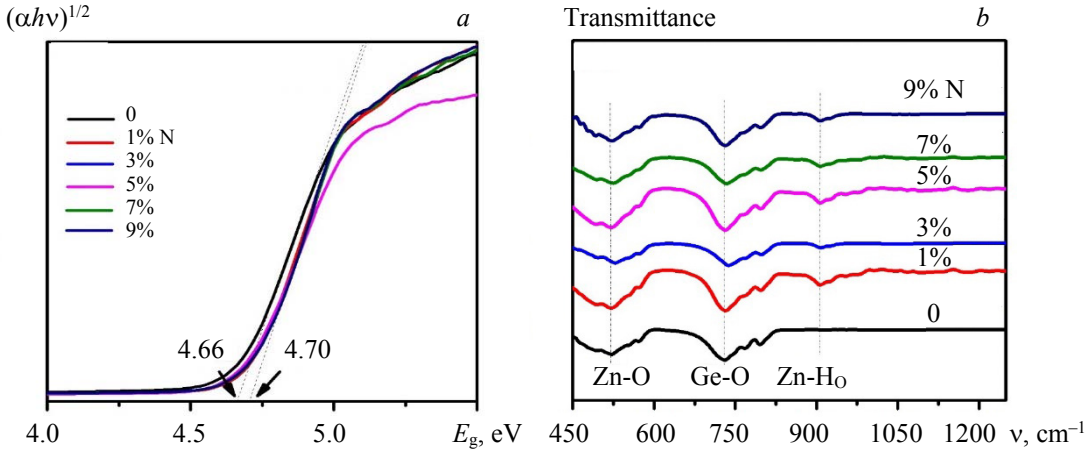

Fig. 3. (a) UV-Vis and (b) FTIR spectra of ZGO:*x* mol.% N (*x* = 0–9) nanophosphors prepared using a hydrothermal method at 200°C for 2 h.

Figures 4a and b show the excitation and emission spectra of the ZGO phosphors. The excitation spectrum monitored at 465 and 510 nm was centered at around 260 nm (Fig. 4a), which can be assigned to the band-to-band transition of the ZGO lattice. As shown in Fig. 4b, under UV excitation, the bluish-white (510 nm for undoped ZGO samples) and blue (465 nm for N-doped ZGO samples) emission was attributed to the native defects presented in the Zn_2GeO_4 host crystal, such as oxygen vacancy, Zn interstitial, Zn vacancy, and

Ge vacancy [19, 20]. This blue shift in the band region emission for nanoparticles, compared with that for undoped, was due to the size-confinement effect for nanoparticles [21]. However, only a small change in band region emission occurred in our case, as the prepared nanoparticles were not too small to experience strong quantum confinement. Therefore, the slight blue shift could be attributed collectively to the emergence of discrete energy states owing to the nanosized structure and insertion of nitrogen defect states within the electronic structure of ZGO. The spectrum was similar, and no peak shift occurred at all. This finding showed that the intensity of fluorescence of N ions in the lattice was maximized when the doping concentration was ~5 mol%, and the phenomenon of fluorescence quenching occurred with increased doping concentration.

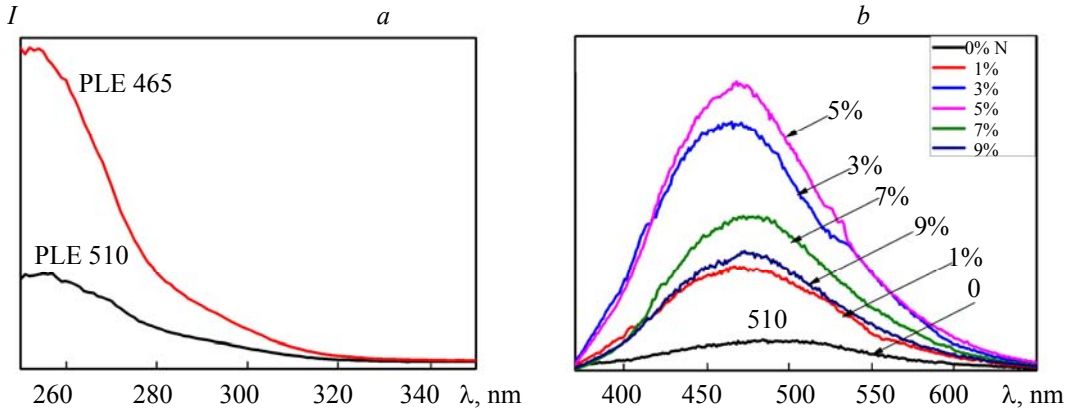

Fig. 4. (a) PLE, (b) PL spectra of ZGO of ZGO:*x* mol.% N (*x* = 0–9).

A published report on N-doped ZnO has revealed that complexes of N_O–V_{Zn} are shallow acceptors [22, 23]. The switching of an N to an O site and leaving a Zn vacancy behind formed a shallow defect complex with high barrier energy. This finding proved that the N defect levels were just above the valance band, and the absorption process brought the N defects state to the deep discrete states in the conduction band. Based on the above results, we established a schematic of the PL mechanism of N-doped ZGO phosphors synthesized using a hydrothermal method, as shown in Fig. 5. Under ultraviolet excitation, the excited electrons were trapped by the defects and then released, with blue emission (~465 nm).

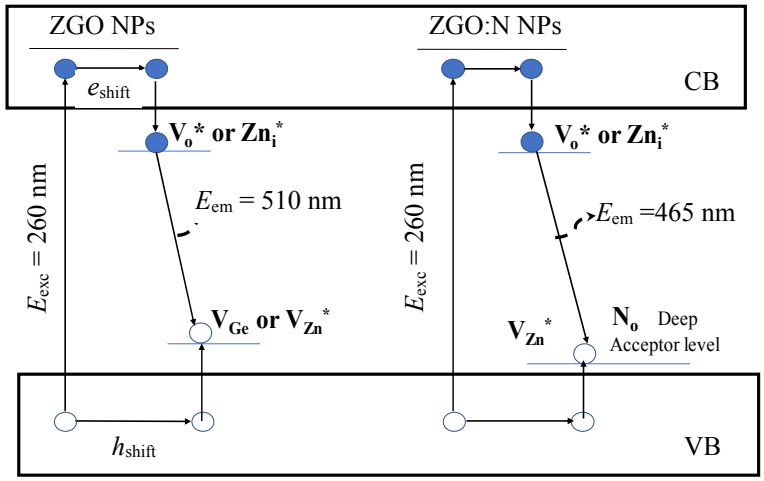

Fig. 5. Photoluminescent mechanism of ZGO:N phosphors prepared using a hydrothermal method.

Conclusions. We successfully synthesized a series of ZGO:*x* mol.% N (*x* = 0–9) nanophosphors using a hydrothermal method to improve the luminescence of defects. The formation of a purely rhombohedral phase for undoped and N doped samples was ascertained through XRD analysis. Owing to N doping, a light blue shift in the energy bandgap from 4.66 to 4.7 eV was observed. Furthermore, the substitution of O by N in the ZGO lattice, confirmed through FTIR analysis wherein ZGO:N was passivated by H, resulted in the occurrence of N_O-H mode. Upon the excitation of 260 nm, the emission spectrum exhibited a broad band in the range 350–600 nm, which was centered at around 510 nm for undoped and 465 nm for N-doped ZGO. The blue shift in emission for phosphors was due to the size-confinement effect for nanoparticles. ZGO:N material is a fluorescent powder with potential application in the production of blue phosphor.

Acknowledgments. This research was funded by the Hanoi University of Science and Technology (HUST) under project number T2020-SAHEP-032.

REFERENCES

1. L. I. Bo, S. Shu-yan, S. U. N. Xiu-juan, P. Jing, W. Bo, X. Yan, *Chem. Res. Chin.*, **28**, 764–767 (2012).
2. Z. Liu, X. Jing L. Wang, *J. Electrochem. Soc.*, **154**, H500 (2007).
3. Y. Li, K. Ding, B. Cheng, Y. Zhang, Y. Lu, *Phys. Chem. Chem. Phys.*, **17**, 5613–5623 (2015).
4. N. M. C. H. P. Lan, C. X. Thang, V.-H. Pham, P. T. Kien, V. T. N. Minh, T. T. H. Tam, *Optik (Stuttg.)*, **199**, 163310 (2019).
5. J. Sato, H. Kobayashi, K. Ikarashi, N. Saito, H. Nishiyama, *J. Phys. Chem. B*, **108**, 4369–4375 (2004).
6. S. Takeshita, J. Honda, T. Isobe, T. Sawayama, S. Niikura, *Cryst. Growth Des.*, **10**, 4494–4500 (2010).
7. Z. Gu, F. Liu, X. Li, Z. W. Pan, *Phys. Chem. Chem. Phys*., **15**, 7488–7493 (2013).
8. Q. Liu, Y. Zhou, J. Kou, X. Chen, Z. Tian, J. Gao, S. Yan, Z. Zou, *J. Am. Chem. Soc.*, **132**, 14385–14387 (2010).
9. M. Shang, G. Li, D. Yang, X. Kang, C. Peng, J. Lin, *Dalton Trans*., **41**, 8861–8868 (2012).
10. Y. Li, A. Zhao, C. Chen, C. Zhang, J. Zhang, G. Jia, *Dyes Pig.*, **150**, 267–274 (2018).
11. Q. Bai, P. Li, Z. Wang, S. Xu, T. Li, Z. Yang, Z. Xu, *Spectrochim. Acta A: Mol. Biomol. Spectr.*, **199**, 179–188 (2018).
12. Q. Bai, Z. Wang, P. Li, S. Xu, T. Li, Z. Yang, *RSC Adv.*, **6**, 102183–102192 (2016).
13. G. Gao, L. Wondraczek, *J. Mater. Chem. C*, **1**, 1952–1958 (2013).
14. R. Kumari, A. Sahai, N. Goswami, *Progress Nat. Sci. Mater. Int.*, **25**, 300–309 (2015).
15. M. Cohen, *Elements of Diffraction*, Addison-Wesley Co. Inc., 459–460 (1956).
16. N. Goswami, D. K. Sharma, *Physica E*, **42**, 1675–1682 (2010).
17. O. Yamaguchi, J. Hidaka, K. Hirota, *J. Mater. Sci. Lett*., **10**, 1471 (1991).
18. S. Limpijumnong, X. Li, S. H. Wei, S. Zhang, *Physica B*, **376**, 686–689 (2006).
19. Z. J. Gu, F. Liu, X. F. Li, Z. W. Pan, *Phys. Chem. Chem. Phys.*, **15**, 7488 (2013).
20. G. J. Gao, L. Wondraczek, *J. Mater. Chem. C Mater. Opt. Electron. Dev.*, **1**, 1952 (2013).
21. J. I. Pankove, *Optical Processes in Semiconductors*, New York, Courier Corporation (2012).
22. A. Boonchun, W. R. Lambrecht, *Phys. Status Solidi b*, **250**, 2091–2101 (2013).
23. S. Lautenschlaeger, M. Hofmann, S. Eisermann, G. Haas, M. Pinnisch, A. Laufer, B. Meyer, *Phys. Status Solidi b*, **248**, 1217–1221 (2011).